Journal of Electronic Testing (2024) 40:5–18
https://doi.org/10.1007/s10836-023-06097-0

An End-to-End Mutually Exclusive Autoencoder Method for Analog Circuit Fault Diagnosis

Yuling Shang[1] · Songyi Wei[1] · Chunquan Li[2] · Xiaojing Ye[1] · Lizhen Zeng[3] · Wei Hu[1] · Xiang He[1] · Jinzhuo Zhou[1]

Received: 26 December 2022 / Accepted: 27 December 2023 / Published online: 16 April 2024

Abstract
Fault diagnosis of analog circuits is a classical problem, and its difficulty lies in the similarity between fault features. To address the issue, an end-to-end mutually exclusive autoencoder (EEMEAE) fault diagnosis method for analog circuits is proposed. In order to make full use of the advantages of Fourier transform(FT) and wavelet packet transform(WPT) for extracting signal features, the original signals processed by FT and WPT are fed into two autoencoders respectively. The hidden layers of the autoencoders are mutually exclusive by Euclidean distance restriction. And the reconstruction layer is replaced by a softmax layer and 1-norm combined with cross-entropy that can effectively enhance the discriminability of features. Finally, the learning rate is adjusted adaptively by the difference of loss function to further improve the convergence speed and diagnostic performance of the model. The proposed method is verified by the simulation circuit and actual circuit and the experimental results illustrate that it is effective.

Keywords Analog circuit · Discriminability · End-to-end mutually exclusive autoencoder · Fault diagnosis · Fourier transform · Wavelet packet transform

1 Introduction

Analog circuits are widely used in national defense, military, aerospace, and so on. When a fault occurs in analog circuits, it can cause partial function failure or performance degradation, and in serious cases, it can even lead to the paralysis of the whole system, so fault diagnosis technology for analog circuits is gradually becoming a hot research topic. Analog circuit faults can be classified as parametric faults and catastrophic faults. Parametric faults refer to device parameters deviating from the normal tolerance range. Catastrophic faults mean open and short in circuits. If parametric faults occur in a circuit, locating it can avoid circuit function failure and even reduce the probability of catastrophic faults. The difference between parametric faults and normal tolerance range is not obvious which will affect the accuracy of fault diagnosis [23]. Therefore, it is very important to extract features with high discriminability.

In analog circuit fault diagnosis, data-driven fault diagnosis methods include two steps: fault feature extraction and fault classification [15]. The methods of fault feature extraction generally include wavelet transform [12, 17], Fourier transform [25], S transform [9], Hilbert-Huang transform [14], and Gabor analysis [10]. But a lot of redundant information is compressing high-dimensional features into low-dimensional features while retaining as much information as possible. Song et al. extracted statistical features from processed signals by using the fractional Fourier transform in the optimal fractional order domain and reduced features dimension through kernel principal components analysis(KPCA),which had a better diagnostic effect compared with the wavelet feature, frequency feature, and conventional time domain feature [11]. He et al. carried out feature dimension reduction through Hilbert-Schmidt independent criterion and Kernel Fischer linear

Responsible Editor: B. C. Kim

✉ Chunquan Li
lcq@guet.edu.cn

[1] Department of Electronic Engineering and Automation, Guilin University of Electronic Technology, Guilin 541000, Guangxi, China

[2] Department of Mechanical and Electrical Engineering, Guilin University of Electronic Technology, Guilin 541000, China

[3] Department of Graduate, Guilin University of Electronic Technology, Guilin 541000, China

discriminant analysis and sent it into a naive Bayes classifier to achieve fault diagnosis [5]. Yuan et al. considered the geometric structure of fault data in a high-dimensional space and proposed a new fault feature dimension reduction algorithm based on locally linear embedding and data mining, and the results showed that it had a good effect on dimension reduction [22]. Arabi et al. extracted features from frequency responses and transient responses for classifier training and used variable dimension reduction to reduce the number of features, different classifiers selected different feature combinations, which had good diagnostic effects [1].

However, the above dimension reduction methods usually lead to information loss. By contrast, deep learning can be utilized to extract deep features and has a strong learning ability [2, 6]. Zhang et al., Zhao et al. and Liu et al. applied the deep belief network in the field of analog circuit fault diagnosis [8, 23, 26], and then Zhang et al. applied particle swarm optimization algorithm in deep belief network to optimize structural parameters and improve performance [24]. Gao et al. proposed the denoising sparse deep autoencoder and adopted linear discriminant analysis for linear dimension reduction to obtain the maximum clustering feature of the signal, but this method failed to make full use of the autoencoder for automatic feature extraction [3]. To improve the training efficiency, Yang et al. proposed a method in which encoders, decoders, and classifiers are trained simultaneously and the maximum clustering characteristics of features are improved [20]. Yang et al. used a one-dimensional convolutional neural network (1D-CNN) to realize the fault diagnosis of fourth-order Butterworth low-pass filter circuit and proved its excellent performance [19]. It can be seen from the above that deep learning has advantages in fault diagnosis.

Most scholars' diagnostic models are applicable when fault value is constant [11, 13, 18, 20], but their effectiveness is not clear when fault value varies within a range. In actual conditions, fault value varies within a range, and compared to the case where fault value is constant, the diagnosis is more difficult.

To address the issue, an end-to-end mutually exclusive autoencoder (EEMEAE) of analog circuits fault diagnosis method is proposed in the paper. Wavelet packet transform and Fourier transform high-level complementary features are extracted by EEMEAE. 1-norm is used to minimize intra-class distance and maximize inter-class distance, combined with cross-entropy to improve the discriminability of features. The convergence speed and diagnostic performance of the model are further improved by adaptive learning rate adjustment. The effectiveness of the proposed method is verified by the four-opamp biquad high-pass filter circuit, and the results show that it is effective.

2 The Proposed Model

2.1 Mutually Exclusive Autoencoder

Different faults are sensitive to different signal processing methods. To extract high-level features of wavelet packet transform (WPT) and Fourier transform (FT), a mutually exclusive autoencoder model is proposed. The mutually exclusive autoencoder model is shown in Fig. 1.

The mutually exclusive autoencoder is composed of two autoencoders with the same structure. The features of the hidden layers are mutually exclusive by maximizing the Euclidean distance. Although the two autoencoders have the same structure, after the wavelet packet transform and Fourier transform are input to the two autoencoders for training, the network weights will be different, so the extracted features will be different.

The wavelet transform features are represented by $x=\{x_1,x_2,x_3,\ldots,x_n\}$. The Fourier transform features are represented by $t=\{t1,t2,t3,\ldots,tn\}$, High-level features extracted from autoencoder are represented by $h=\{h_1,h_2,h_3,\ldots h_m\}$, W_e is a weight matrix and b_e is a bias vector. It can be obtained by formula (1)

$$h = f_e\left(W_e x + b_e\right) \tag{1}$$

The autoencoder network weights are adjusted by minimizing the input samples and reconstructing errors. Reconstructed samples can be obtained by the decoder, and reconstructed samples are represented by $z=\{z_1,z_2,z_3,\ldots z_n\}$. W_d is a weight matrix and b_d is a bias vector. It can be obtained by formula (1)

$$z = f_{ae}(W_d h + b_d) \tag{2}$$

The mutually exclusive hidden layers are represented by the following formula (3).

$$M = \|h_1 - h_2|^2 - D| \tag{3}$$

h_1 and h_2 respectively represent the high-level features of wavelet packet transform and Fourier transform, D is a

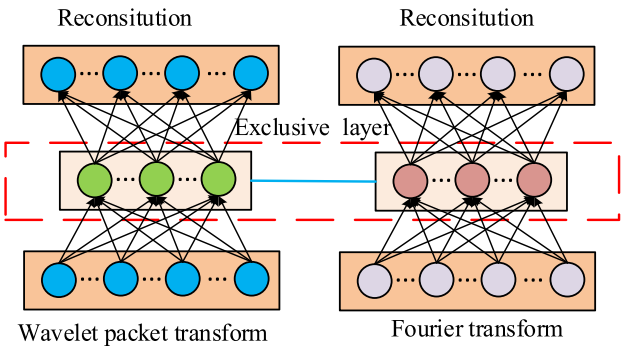

Fig. 1 Mutually exclusive autoencoder

number greater than zero. When the difference between the Euclidean distance of h_1 and h_2 and D is decreased, the Euclidean distance of h_1 and h_2 increases.

To extract high-level complementary features of wavelet packet transform and Fourier transform, the loss function is shown in (4).

$$Y = ae_w + bM + ce_f \tag{4}$$

The e_w and e_f are the reconstructed errors of wavelet packet transform and Fourier transform respectively, and M achieves mutual exclusion between features. a, b and c are coefficients used to control the proportion of reconstruction error and mutually exclusive features.

2.2 An End-to-End Mutually Exclusive Autoencoder for Analog Diagnosis

The fault features of analog circuits are very similar, However, the traditional autoencoder uses the reconstructed error as the loss function. It blurs the distinguishability between classes. To extract distinguishable features, a new joint 1-norm and cross-entropy loss function is proposed.

$$E = \sum_{i=1}^{N}\sum_{j=1}^{N} \|h_1 - h_j| - S_{ij}| \tag{5}$$

S_{ij} is used to limit the 1-norm between the features of the hidden layer. If the training samples x_i and x_j are the same label $S_{ij}=0$; If the training samples x_i and x_j are different labels $S_{ij}=c$, c is a number greater than zero. When the optimizer is introduced to minimize the loss function, if the training samples are the same label, $|h_i\text{-}h_j|$ will be minimized to make the same fault class features more compact. If training sample labels are different, $||h_i\text{-}h_j|\text{-}S_{ij}|$ will be minimized. The S_{ij} is a number greater than zero, $|h_i\text{-}h_j|$ closes to S_{ij} to increase the distance between classes making different fault class features more distinguishable.

To further improve the feature distinguishability, the softmax classifier is introduced to calculate the cross entropy of hidden layer features. The probability that the *ith* input sample features belong to the type *j* fault is shown in (6), and the cross entropy can be calculated as shown in (7).

$$P_j = \frac{e^{f_j^i}}{\sum_j e^{f_i^j}} \tag{6}$$

$$L = \sum_{i=1}^{N}\sum_{J=1}^{N} y_i^j \log P_j \tag{7}$$

The joint 1-norm and cross-entropy loss function are introduced into the mutually exclusive autoencoder to construct EEMA model, whose loss function is shown in (8)

$$\min J(\theta) = \alpha L + \beta E + \gamma M \tag{8}$$

The end-to-end mutually exclusive autoencoder model uses the gradient descent algorithm and the backpropagation algorithm to adjust the network weights, to obtain the abstract features in the sample. The weights and bias of the autoencoder receiving the wavelet packet transform feature set are respectively

$$W_w = W_w - \eta_1 \frac{\partial J(\theta)}{\partial W_w} \tag{9}$$

$$b_w = b_w - \eta_1 \frac{\partial J(\theta)}{\partial b_w} \tag{10}$$

W_w is a weight matrix, b_w is a bias vector, and η_1 is a learning rate.

The connection weights and bias of the autoencoder receiving the Fourier transform feature set are respectively

$$W_f = W_f - \eta_2 \frac{\partial L}{\partial W_f} \tag{11}$$

$$b_f = b_f - \eta_2 \frac{\partial L}{\partial b_f} \tag{12}$$

W_f is a weight matrix, b_f is a bias vector, and η_2 is a learning rate.

2.3 Adaptive Learning Rate Adjustment

The learning rate plays an important role in weights and bias updates. Li et al. used a particle swarm algorithm to optimize the learning rate of deep belief network, and used diagnosis accuracy as the particle swarm fitness function [7], This method requires training model in each iteration, which leads to optimization time being long.

To avoid the above problem, an adaptive learning rate adjustment method is introduced. Haidong et al. improve the convergence speed of the algorithm through the difference of loss function adjustment [4], however, this method is limited. When the loss function enters the plain area (the loss function value hardly changes), the learning rate tends to be unchanged. In order to solve this problem, the attenuation mechanism was introduced to make it jump out of the plain area. Frequent updates of learning rates do not take full advantage of the optimal learning rate in the phase, a holding

mechanism was introduced. When the loss function decline value was greater than the threshold (the threshold is set in advance), the learning rate was kept unchanged.

$$\eta(t+1) = (1+\mu) * \eta \tag{13}$$

$$\mu = N * (1 - e^{E(t+1)-E(t)}) \tag{14}$$

N is the tracking coefficient, $E(t+1)$ and $E(t)$ denote the value of the loss function at iterations $t+1$ and t.

2.4 Fault Diagnosis Flow

In this paper, an end-to-end mutually exclusive autoencoder (EEMEAE) fault diagnosis method for analog circuits is proposed. The framework diagram of the proposed method is shown in Fig. 2, and the algorithm flow is described as follows.

Step 1: PSPICE is used for circuit simulation, the faults are injected for Monte Carlo analysis, and time domain signals of all fault classes in the output are measured and saved.

Step 2: The time domain signals are processed by wavelet packet transform and Fourier transform, and they are split into the training set and the testing set.

Step 3: The original signals are sent to the autoencoder 1 after Fourier transform. The reconstruction layer is removed and a softmax layer is introduced. The difference between the cross entropy of the last iteration and the cross entropy of the current iteration is calculated to adjust the learning rate.

Step 4: The original signals are sent to the autoencoder 2 after wavelet packet transform. The reconstruction layer of the autoencoder is removed, the loss function of joint 1-norm and cross-entropy is introduced, and the hidden layer features of the autoencoder1 and the autoencoder2 trained in Step3 are mutually exclusive.

Step 5: When the number of iterations is reached, the training is terminated to obtain the best network parameters and save.

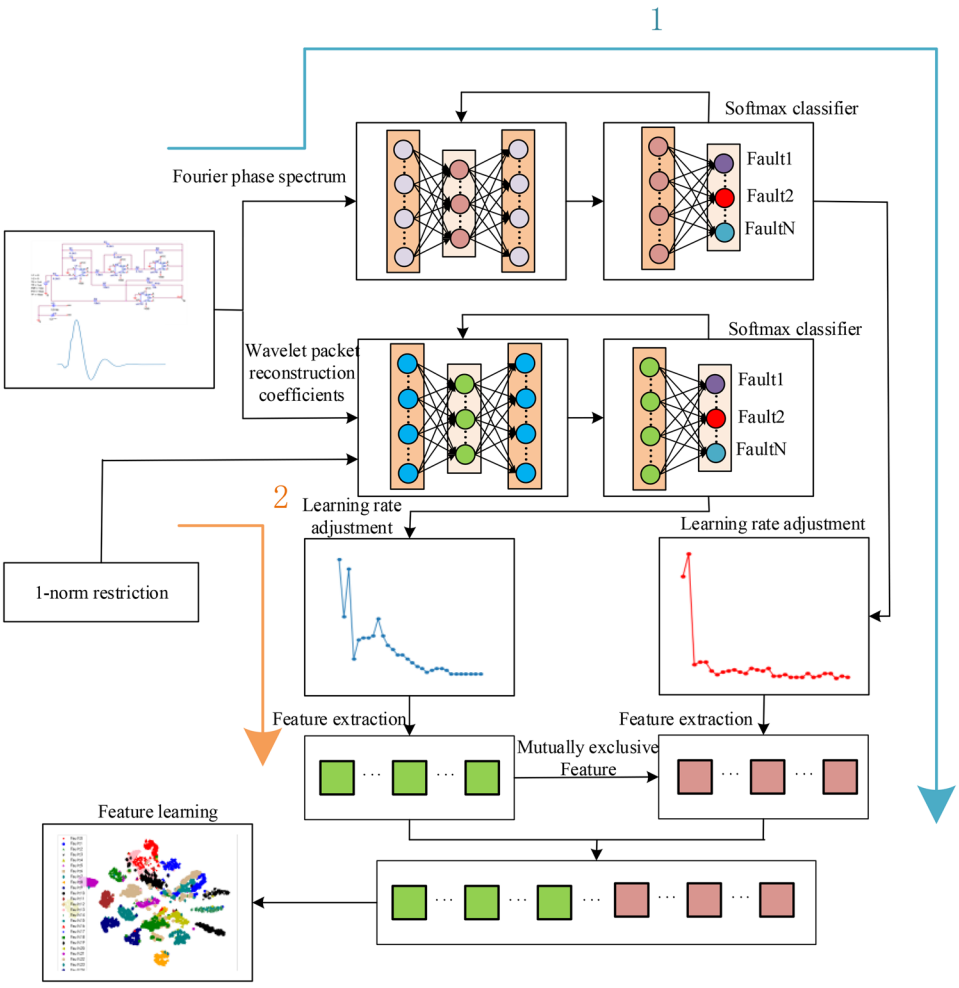

Fig. 2 Frame diagram of the proposed method

Step 6: The features extracted by the EEMEAE are fed into the support vector machine (SVM) classifier and then testing samples are verified for the effectiveness of the proposed model.

3 Experiment and Analysis

In the actual situation, the single fault of probability is much higher than that of multiple faults [19]. Therefore, only a single fault is considered in the paper. The tolerance of resistors and capacitors is set to 5% and 10% [3]. The deviation of component parameters from the nominal value to [20%, 50%] is considered a soft fault.

3.1 Fault Set Establishment

In this paper, the four-opamp biquad high-pass filter circuit is selected as the circuit under test (CUT), as shown in the Fig. 3. The excitation source is a pulse with an amplitude of 5 V, a rise time of 1us, a duration of 10us, a frequency of 1 kHz, and a fall time of 10us.

The four-opamp biquad high-pass filter circuit contains 12 components, and a component includes two kinds of faults. All kinds of fault modes are shown in the Table 1, ↑ which indicates the parameter value rises, ↓ indicates the parameter value falls, and NF indicates a normal state.

Table 1 Fault category

Fault Code	Fault Class	Nominal Value	Fault Range
1	R1↑	6.2kΩ	[6.82 k,9.3 k]
2	R1↓	6.2kΩ	[3.1 k,5.58 k]
3	R2↑	6.2kΩ	[6.82 k,9.3 k]
4	R2↓	6.2kΩ	[3.1 k,5.58 k]
5	R3↑	6.2kΩ	[6.82 k,9.3 k]
6	R3↓	6.2kΩ	[3.1 k,5.58 k]
7	R4↑	1.6kΩ	[1.76 k,2.4 k]
8	R4↓	1.6kΩ	[0.8 k,1.44 k]
9	C1↑	5nF	[5.5n,7.5n]
10	C1↓	5nF	[2.5n,4.5n]
11	C2↑	5nF	[5.5n,7.5n]
12	C2↓	5nF	[2.5n,4.5n]
13	NF	-	-
14	R5↓	5.1kΩ	[2.55 k,4.55 k]
15	R5↑	5.1kΩ	[5.61 k,7.61 k]
16	R6↓	5.1kΩ	[2.55 k,4.55 k]
17	R6↑	5.1kΩ	[5.61 k,7.61 k]
18	R7↓	10kΩ	[5.00 k,9.00 k]
19	R7↑	10kΩ	[11.00 k,15.00 k]
20	R8↓	10kΩ	[5.00 k,9.00 k]
21	R8↑	10kΩ	[11.00 k,15.00 k]
22	R9↓	10kΩ	[5.00 k,9.00 k]
23	R9↑	10kΩ	[11.00 k,15.00 k]
24	R10↓	10kΩ	[5.00 k,9.00 k]
25	R10↑	10kΩ	[11.00 k,15.00 k]

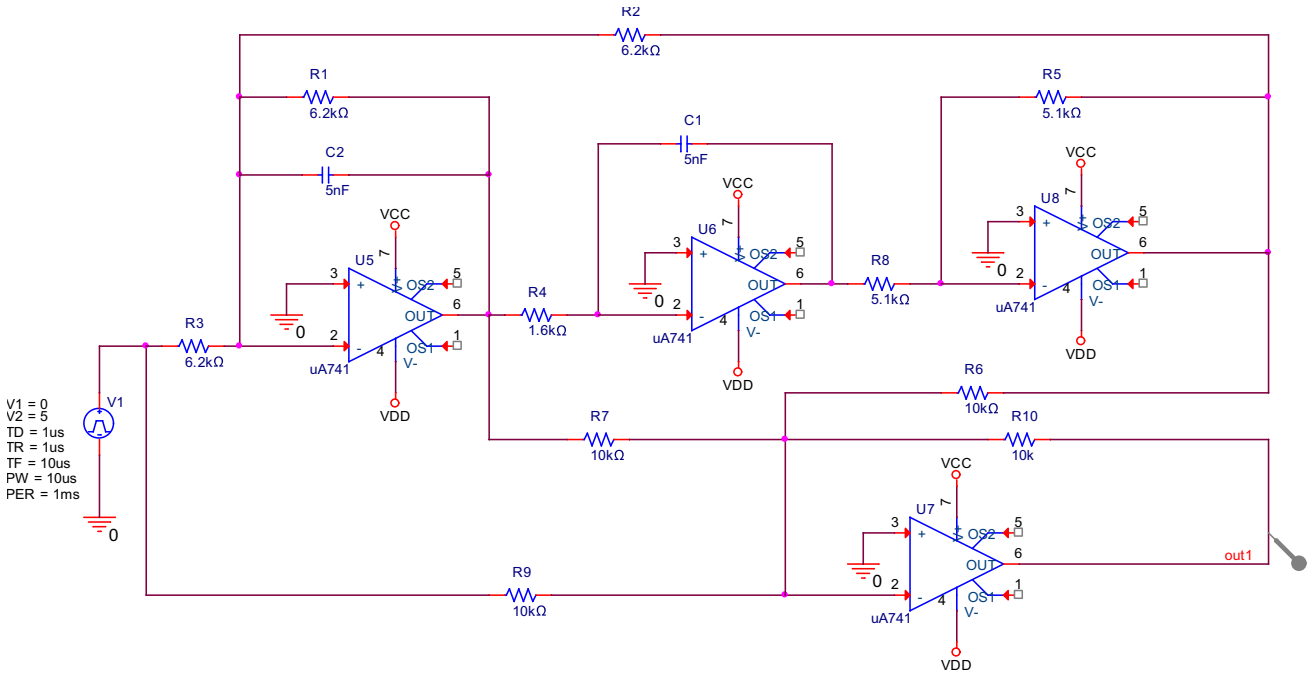

Fig. 3 Four-opamp biquad high-pass filter circuit

The excitation was input to CUT, and the time signals within 1 ms-1.4 ms of all fault types were collected at the output. The sampling time interval was 1us, so 400 sampling points are collected from each signal. Monte Carlo analysis is used to generate 300 signals for each fault, 200 signals are selected as the training set, and the remaining 100 signals are selected as the testing set.

3.2 Fault Diagnosis and Classification

Through sensitivity analysis, the output voltage is more sensitive to the components *R1*, *R2*, *R3*, *R4*, *C1*, and *C2*. A fault set containing 13 fault modes can be constructed, and the fault codes are from 1 to 13, as shown in Table 1 fault category.

The network structure of the autoencoder is 400-135-101-56-*X*, and there are three hidden layers. The number of neurons in the hidden layers is 135, 101, and 56 respectively.

The number of neurons in the input layer is 400 depending on the number of sampling points, and the number of neurons in the output layer is *X* depending on the number of fault types. The initial learning rate is 0.01.

To verify the effectiveness of the proposed method, all fault classes are mapped on a two-dimensional feature map by T-SNE clustering visualization. Fault classes of the original data are mixed. After EEMEAE feature extraction, the different fault modes have a high distinguishability. It is shown in Figs. 4, 5, 6, and 7.

To further evaluate the performance of fault diagnosis, each fault mode is classified by SVM. SVM is used without any optimization in the sklearn library. It can be seen from the confusion matrix Figs. 8 and 9 that the fault classification is correct.

Most scholars only consider the fault of sensitive components in analog circuit fault diagnosis. To reflect the superiority of the proposed method in the paper, all the components of the circuit are considered, which contains a total of 25 kinds of faults as shown in Table 1. All fault classes are mapped on a two-dimensional feature map by T-SNE clustering visualization.

3.3 Comparison and Discussion

When only considering the fault of sensitive components, the proposed method improves the fault diagnosis accuracy to 100%, which is significantly higher than the fault diagnosis accuracy of other methods, as shown in Table 2.

Other methods consider only the case where the fault value is constant. In the paper, the case where fault value varies within a range is considered. It is compared with the case of the same fault degree, the diagnosis is more difficult.

When the case where the fault value varies within a range is considered in the other methods, the diagnosis accuracy of the proposed methods is higher, as shown in Table 3. Although the CUT is different, the number of fault types in this paper is the highest. The range of faults in this paper is the largest, the fault range is [10%, 50%]. However, The fault ranges of DBN-CPSO [23], S3VM [16], and Bispectral Models [21] are [5%, 25%], [30%, 50%] and [10%, 20%], respectively.

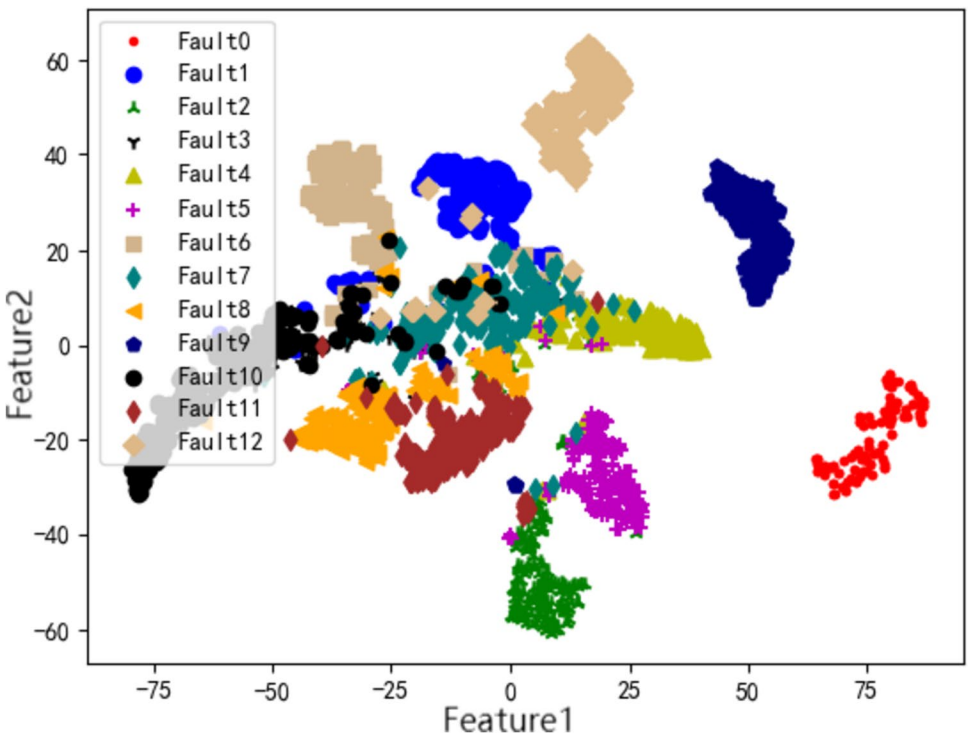

Fig. 4 Original data visualization (13 fault types)

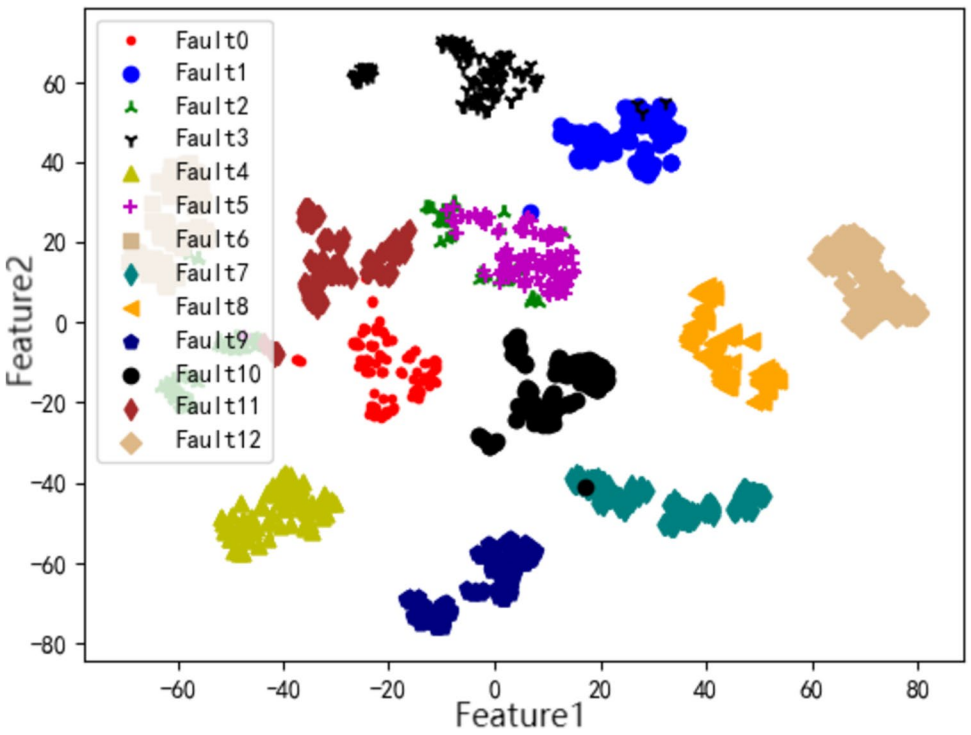

Fig. 5 Feature visualization after feature extraction (13 fault types)

To further verify the validity of the proposed method, the time domain signal is processed by Fourier transform and wavelet packet transform, and they are combined into a long vector. Long vectors are fed into autoencoder called Fourier Wavelet autoencoder (FWAE), Fourier transform is fed into autoencoder called Fourier autoencoder (FTAE),

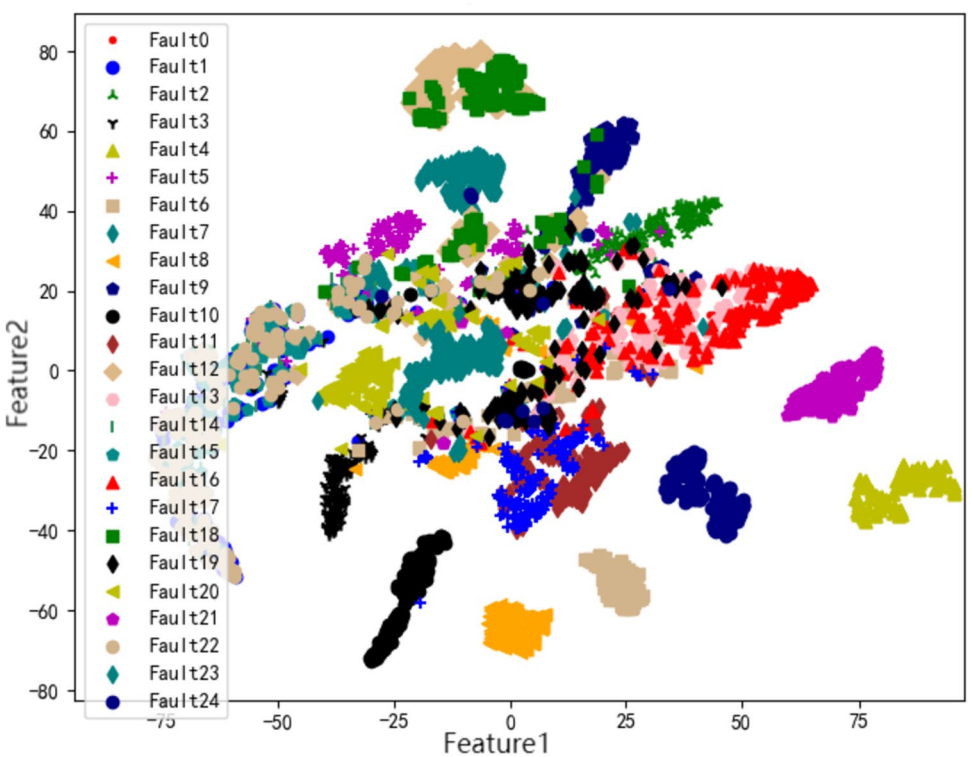

Fig. 6 Original data visualization (25 fault types)

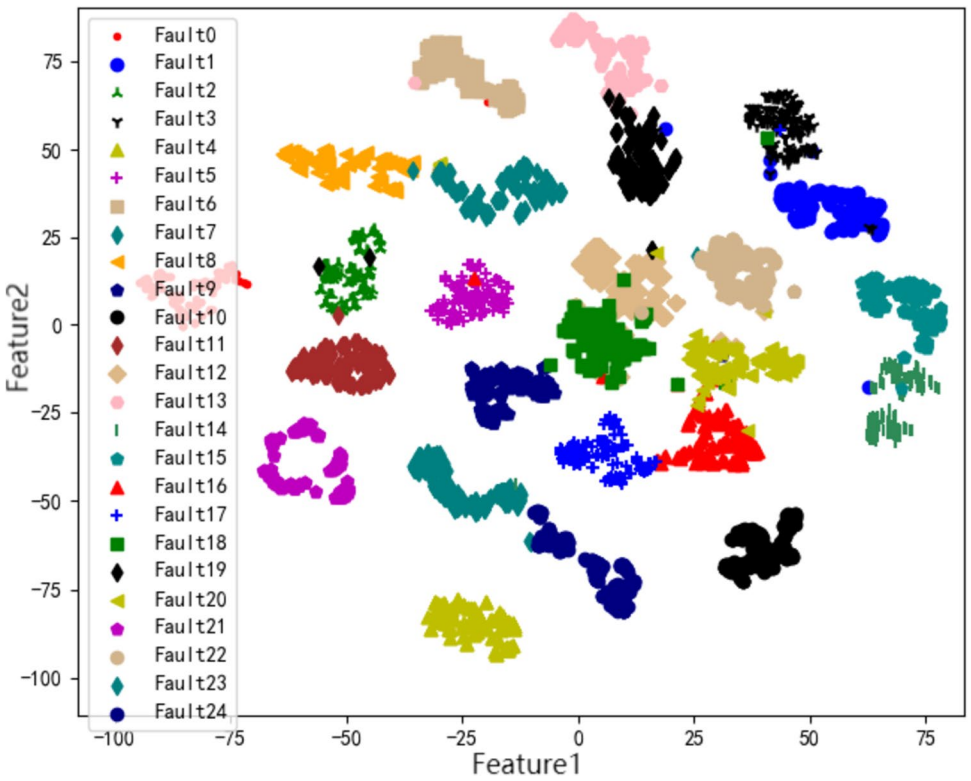

Fig. 7 Feature visualization after feature extraction (25 fault types)

wavelet packet transform is fed into autoencoder called wavelet packet autoencoder (WPAE). In the training set, the number of correctly classified samples of the 25 fault types is shown in Fig. 10. The fault diagnosis accuracy of FTAE is 98.3%, WPAE is 75.26%, FWAE is 97.9%, and EEMEAE is 99.76%.

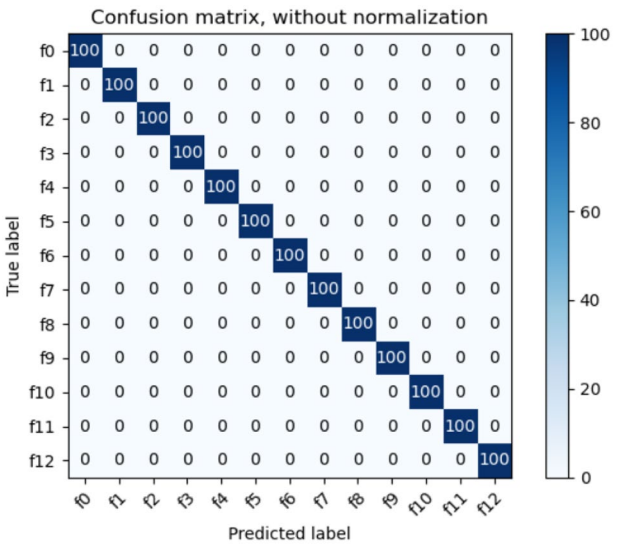

Fig. 8 Confusion matrix (13 fault types)

In the testing set, the number of correctly classified samples is shown in Fig. 11. The diagnosis accuracy of FTAE, WPAE, FWAE, and EEMEAE is 64.76%, 75.08%, 97.6%, and 99.64%, respectively. In the training set, the diagnosis accuracy of FTAE is second only to the EEMEAE, but in the testing set, the diagnosis accuracy of FTAE decreases significantly. It can be seen that the fault diagnosis cannot be accurately carried out only by wavelet packet transform or Fourier transform. Both in the training set and the testing set, the diagnosis accuracy of EEMEAE is the highest. FWAE and EEMEAE input data and structural parameters are the same, which further verifies the effectiveness of EEMEAE.

The component values of analog circuits are continuous, so there are infinite fault values in a fault range. Therefore, good fault diagnosis performance in the case of insufficient training samples is great significance in analog circuit fault diagnosis. To verify the generalization performance of the proposed model, change the training sample proportion in all samples, it can be seen that, no matter how much the proportion of the training sample, the diagnosis accuracy rate of EEMEAE is always higher than the diagnosis accuracy of FWAE. When the training sample proportion is 40%, the diagnosis accuracy rate has reached 98.13%, which shows that EEMEAE has good generalization performance as shown in Fig. 12.

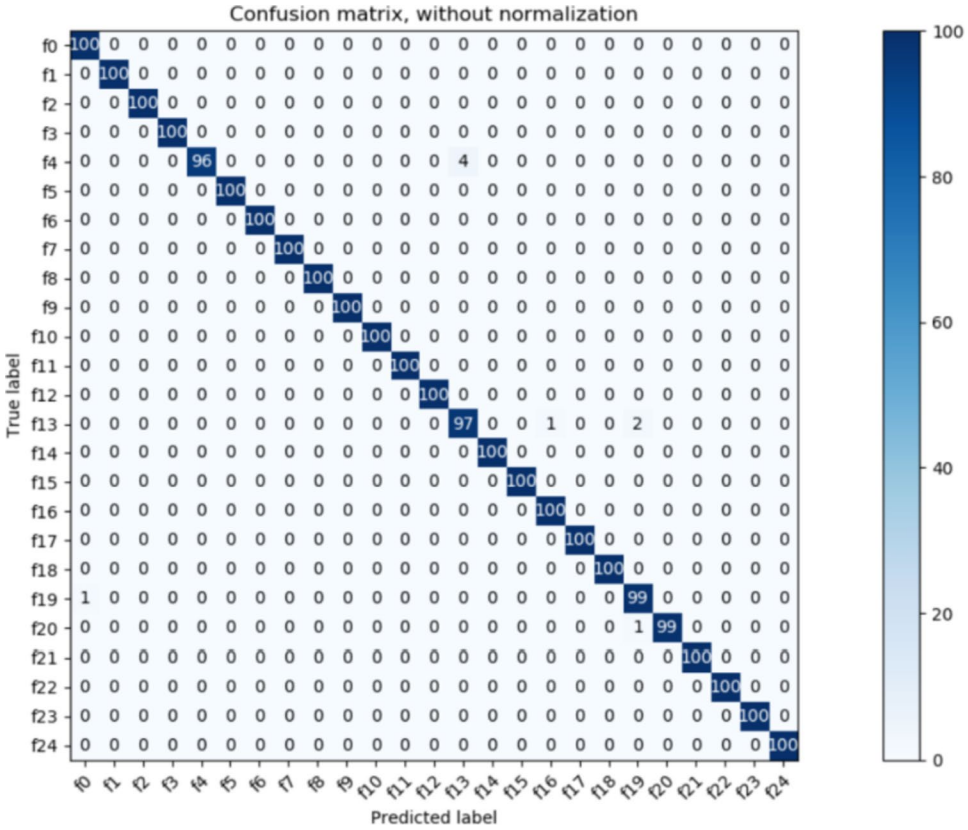

Fig. 9 Confusion matrix (25 fault types)

The effectiveness of the adaptive learning rate adjustment strategy can be illustrated by Figs. 13 and 14. It can be seen that the adaptive learning rate adjustment can accelerate the convergence speed and loss function value is lower with the same number of iterations.

3.4 Experimental Verification

To verify the practicability of the proposed method, the method is applied to an actual circuit of four-opamp biquad high-pass filter, as shown in Fig. 15.

The signal generator generates a pulse with an amplitude of 5 V, a duration of 20us, and a frequency of 1 kHz. *R1, R2, R3, R4, R5, R6, R7, R8, R9,* and *R10* are selected as fault components respectively, and a total of 20 fault types are set. The parameter values of each fault implant component are shown in Table 1. When there is a fault in *R2*, the waveform is shown in Fig. 16.

Each fault type collects 50 data, 25 data are selected as training samples and the remaining 25 data are selected as testing samples. After feature extraction by EEMEAE, SVM is used for classification. As can be seen from Fig. 17, the fault diagnosis accuracy is 99.2%.It can be seen that the method can be used not only in the simulation circuit but also in the actual circuit.

Table 2 Comparison of fault diagnosis results (13 fault types)

Method	Classes	Accuracy
ANFIS [1]	13	96.74%
DBN-GWO-SVM [13]	13	99.68%
FRFT-KPCA-SVM [11]	13	95.12%
Wavelet-fractal+ridgelet-NN [18]	13	98.52%
EEDAE [20]	13	99.27%
Proposed method	13	100%

Table 3 Comparison of fault diagnosis results

Method	Classes	Accuracy
DBN-CPSO [23]	15	98.13%
S3VM [16]	15	94.1%
Bispectral Models [21]	20	92%
Proposed method	25	99.64%

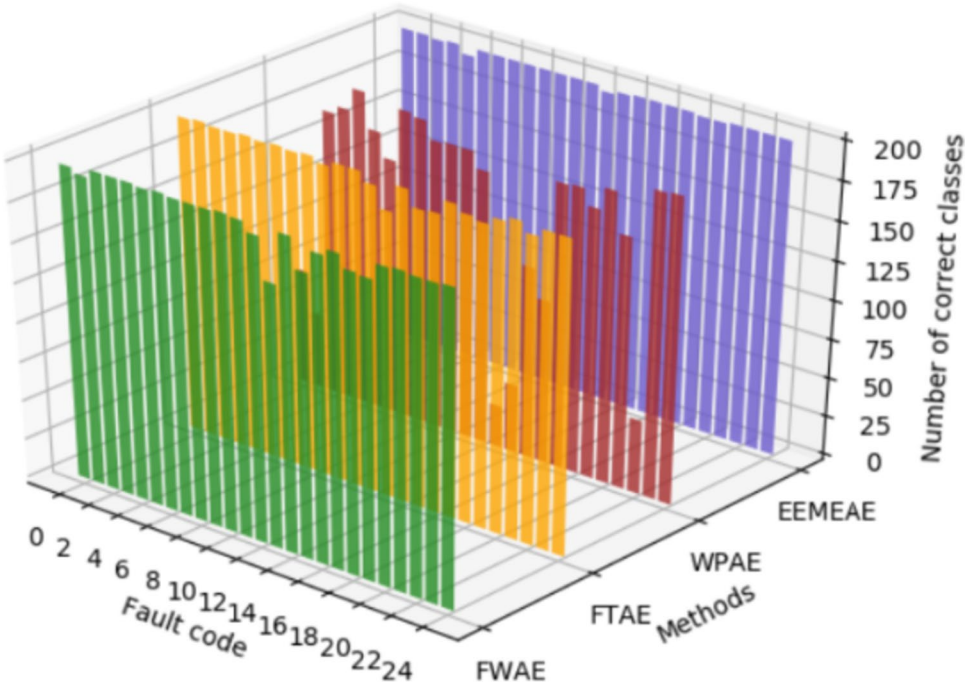

Fig. 10 Fault diagnosis results of the training set

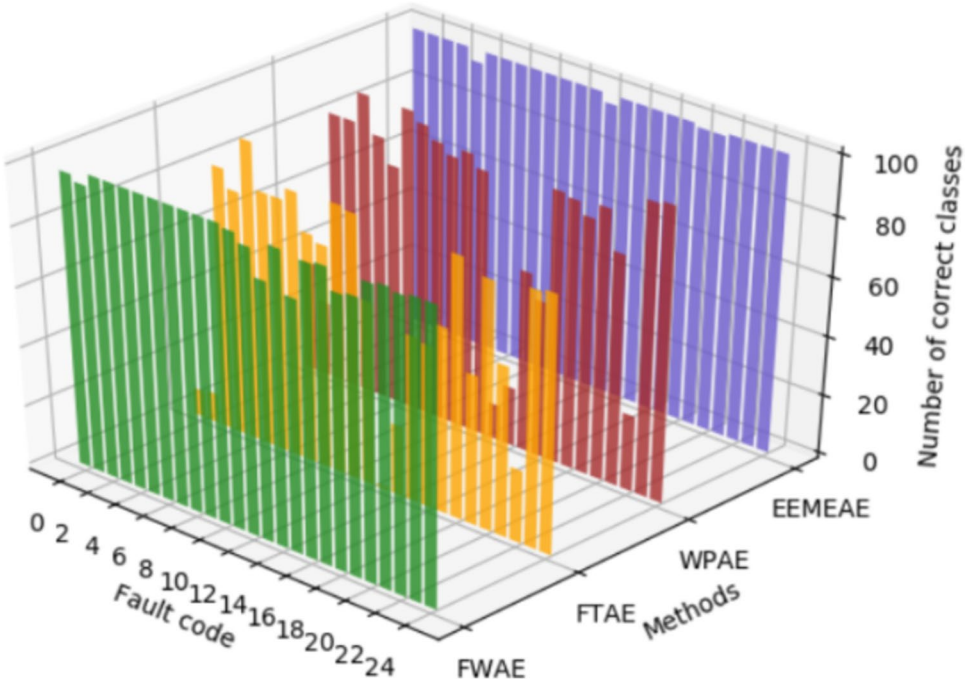

Fig. 11 Fault diagnosis results of the testing set

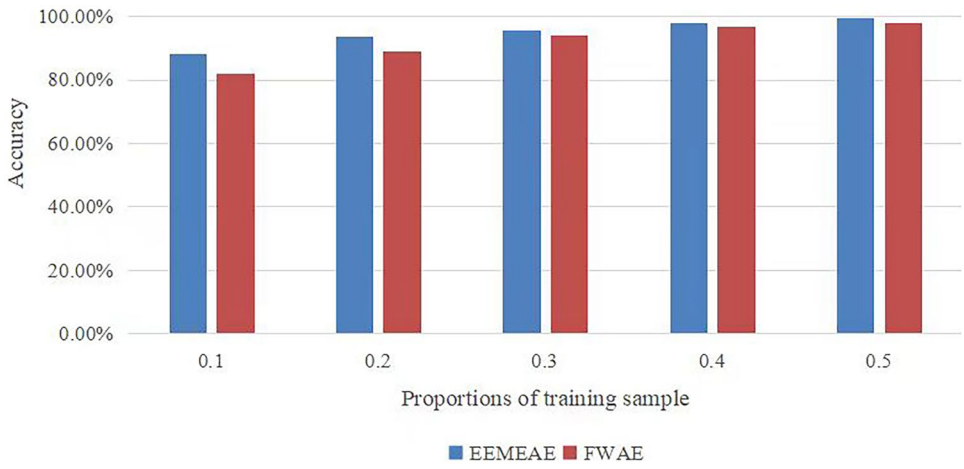

Fig. 12 Fault diagnosis results of different proportions of training samples

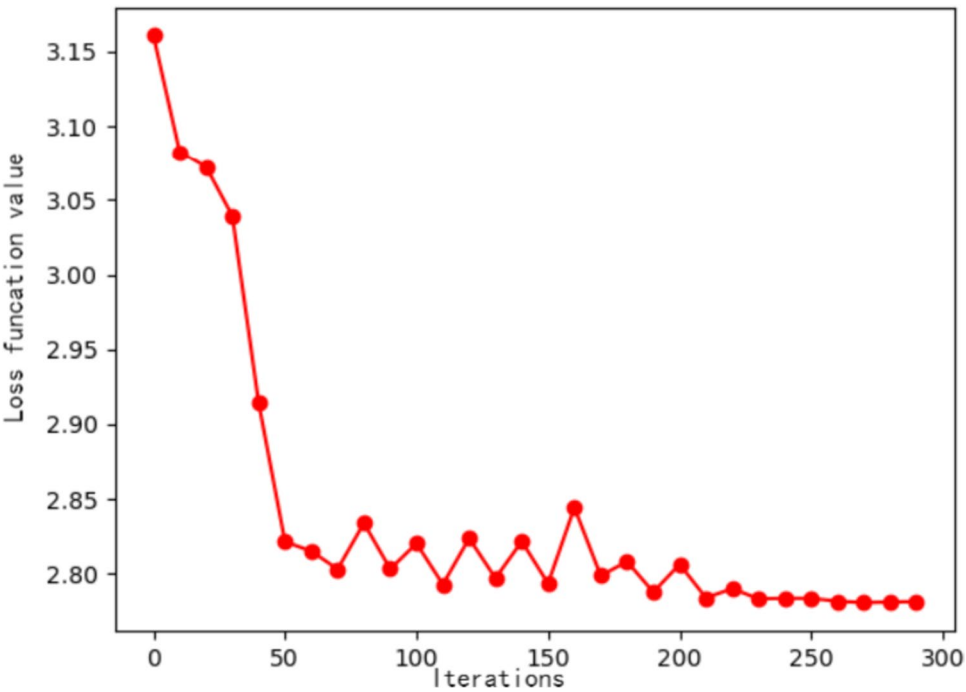

Fig. 13 The loss function curve of adaptive learning rate adjustment

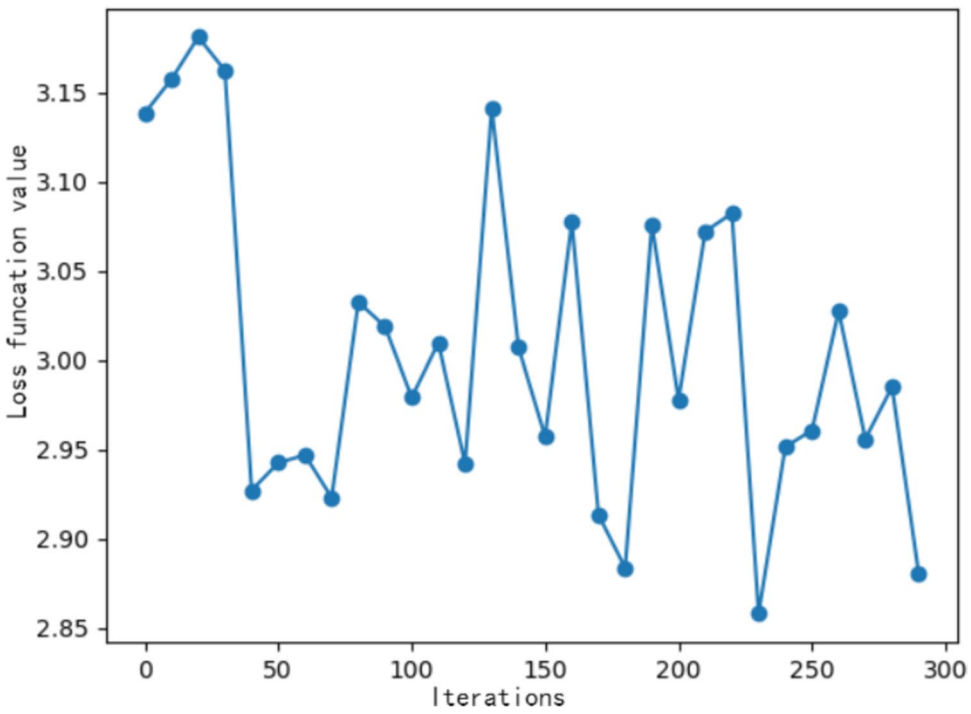

Fig. 14 The loss function curve of learning rate = 0.001

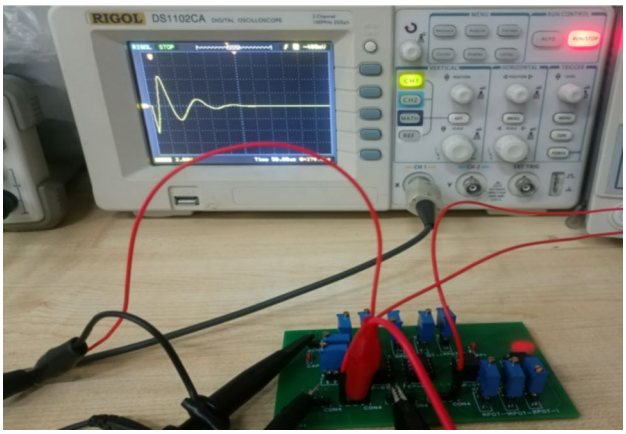

Fig. 15 Actual circuit of four-opamp biquad high-pass filter

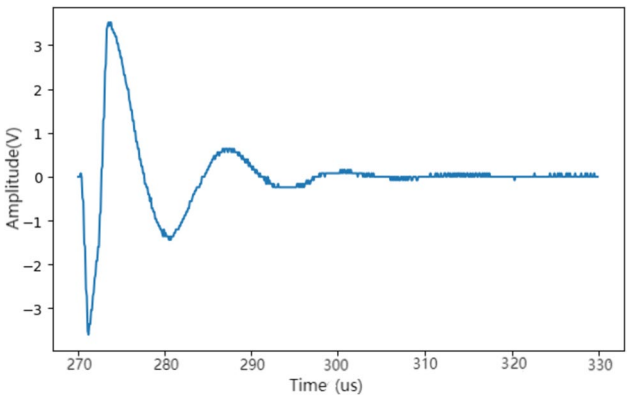

Fig. 16 *R2* fault waveform in the actual circuit

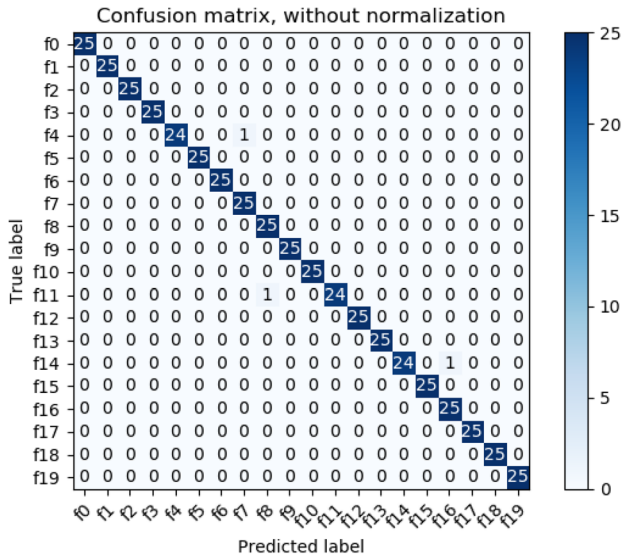

Fig. 17 Confusion matrix (Actual circuit)

4 Conclusion

An end-to-end mutually exclusive autoencoder (EEMEAE) fault diagnosis method for analog circuits is proposed in this paper. The method uses two autoencoders to extract high-level features of Fourier transform and wavelet packet transform. In the loss function, Euclidean distance is used to realize mutual exclusion between features, and 1-norm and cross-entropy are combined to enhance the discriminability of features. To improve the convergence speed, the adaptive learning rate adjustment strategy is introduced. The effectiveness of the proposed method has been demonstrated through the four-opamp biquad high-pass filter circuit. In the simulation circuit, the fault diagnosis accuracy is higher by comparing with other fault diagnosis models. In the actual circuit, the fault diagnosis accuracy is excellent. In summary, the proposed method makes analog circuits maintainability better.

Author Contribution All authors contributed to the study conception and design.

Funding This work is supported by the National Natural Science Foundation of China [No.61661013] and Innovation Project of GUET Graduate Education [2021YCXS132 and YCSW2022281]. (Corresponding author: Chunquan Li).

Availability of Data and Materials The processed data and material required to reproduce these findings cannot be shared at this time as the data also fo-rm part of an ongoing study.

Code Availability Not applicable.

Declarations

Ethics Approval Not applicable.

Consent to Participate All authors approved the version to be published and agree to be accountable for all aspects of the work in ensuring that questions related to the accuracy or integrity of any part of the work are appropriately investigated and resolved.

Consent for Publication All authors approved the final manuscript and the s-ubmission to this journal.

Conflict of Interest The authors declare that there is no conflict of interest or competing interest.

References

1. Arabi N, Bourouba A. Belaout, Ayad M (2019) An accurate classifier based on adaptive neuro-fuzzy and features selection techniques for fault classification in analog circuits. Integration 64:50–59. https://doi.org/10.1016/j.vlsi.2018.08.001
2. Fang F, Li L, Gu Y et al (2020) A novel hybrid approach for crack detection. Pattern Recogn 107:107474. https://doi.org/10.1016/j.patcog.2020.107474
3. Gao T (2021) A novel fault diagnosis method for analog circuits with noise immunity and generalization ability. Neural Comput Appl 33:10537–11055. https://doi.org/10.1007/s00521-021-05810-4
4. Haidong S, Hongkai J, Ke Z, Dongdong W, Xingqiu L (2018) A novel tracking deep wavelet autoencoder method for intelligent fault diagnosis of electric locom-otive bearings. Mech Syst Signal Process 110:193–209. https://doi.org/10.1016/j.ymssp.2018.03.011
5. He W, He Y, Li B, Zhang C (2020) A Naive-Bayes-Based Fault Diagnosis Approach for Analog Circuit by Using Image-Oriented Feature Extraction and Selection Technique. IEEE Access 8:5065–5079. https://doi.org/10.1109/ACCESS.2018.2888950
6. Li F, Long Z, He P, Feng P (2020) Fully convolutional Pyramidal networks for semant-ic segmentation. IEEE Access 8:229132–229140. https://doi.org/10.1109/ACCES-S.2020.3045280
7. Li Y, Wang L, Jiang L (2020) 'Rolling bearing fault diagnosis based on DBN algorithm improved with PSO.' J Vibration and Shock 39(5):89–96. https://doi.org/10.13465/j.cnki.jvs.2020.05.012
8. Liu Z, Jia Z, Vong C-M, Han J (2017) Capturing High-Discriminative Fault F-eatures for Electronics-Rich Analog System via Deep Learning. IEEE Trans Industr Inform 13(3):1213–1226. https://doi.org/10.1109/TII.2017.2690940
9. Mishra PK, Yadav A, Pazoki M (2018) A novel fault classification scheme f-or series capacitor compensated transmission line based on bagged tree ensemble classifier. IEEE Access 6:27373–27382. https://doi.org/10.1109/ACCESS.2018.2836401
10. Riera-Guasp M, Pineda-Sanchez M, Perez-Cruz J, Puche-Panadero R, Roger-Folch J, Antonino-Daviu JA (2012) Diagnosis of induction motor faults via Gabor analysis of the current in transient regime. IEEE Trans Instrum Meas 61(6):1583–1596. https://doi.org/10.1109/TIM.2012.2186650
11. Song P, He Y, Cui W (2016) Statistical property feature extraction based on FRFT for fault diagnosis of analog circuits. Analog Integr Circ Sig Process 87(3):427–436. https://doi.org/10.1007/s10470-016-0721-5

12. Srimani S, Ghosh K, Rahaman H (2020) Wavelet Transform based fault diagnosis in analog circuits with SVM classifier. In 2020 IEEE International Test Conference India (pp. 1–10)
13. Su X, Cao C, Zeng X, Feng Z, Wu Z (2021) Application of dbn and gwo-svm in analog circuit fault diagnosis. Sci Rep 11(1):7969. https://doi.org/10.1038/s41598-021-86916-6
14. Tang S, Li Z, Chen L (2015) Fault detection in analog and mixed-signal circuits by using Hilbert-Huang transform and coherence analysis. Micro Electron J 46(10):893–899. https://doi.org/10.1016/j.mejo.2015.07.004
15. Vasan Sai Sarathi, Long B, Pecht M (2013) Diagnostics and Prognostics Meth-od for Analog Electronic Circuits. IEEE Trans Ind Electron 60(11):5277–5291. https://doi.org/10.1109/TIE.2012.2224074
16. Wang L (2021) Soft fault diagnosis of analog circuits based on semi-supervised support vector machine. Analog Integrated Circuits and Signal Processing 228–228. https://doi.org/10.1007/s10470-021-01851-w
17. Wang L, Zhou D, Tian H, Zhang H, Zhang W (2019) Parametric Fault Diagn-osis of Analog Circuits Based on a Semi-Supervised Algorithm. Analog Integr Circ Sig Process 98:517–526. https://doi.org/10.3390/sym11020228
18. Xiao Y (2012) A novel linear ridgelet network approach for analog fault diagnosis usi-ng wavelet-based fractal analysis and kernel PCA as preprocessors. Measurement 45(3):297–310. https://doi.org/10.1016/j.measurement.2011.11.018
19. Yang H, Meng C, Wang C (2020) Data-Driven Feature Extraction for Analog Ci-rcuit Fault Diagnosis Using 1-D Convolutional Neural Network. IEEE Access 8:18305–18315. https://doi.org/10.1109/ACCESS.2020.2968744
20. Yang Y, Wang L, Chen H, Wang C (2021) An end-to-end denoising autoencoder-based deep neural network approach for fault diagnosis of analog circuit. Analog Integr Circ Sig Process 107(3):605–616. https://doi.org/10.1007/s10470-021-01835-w
21. Yong D, Ning L (2017) Soft fault diagnosis in analog circuits based on bispectral models. J Electron Test 33:543–557. https://doi.org/10.1007/s10836-017-5686-5
22. Yuan Z et al (2018) An efficient feature extraction approachbased on manifold lea-rning for analogue circuits fault diagnosis. Analog Integr Circ Sig Process 102:237–252. https://doi.org/10.1007/s10470-018-1377-0
23. Zhang C, He Y, Du B (2019) Analog circuit incipient fault diagnosis method based on DBN feature extraction. Chin J Scientific Instrument 40:112–119. https://doi.org/10.19650/j.cnki.cjsi.J1905283
24. Zhang C, He Y, Yuan L, Xiang S (2018) Analog Circuit Incipient Fault Diagnosis Method Using DBN Based Features Extraction. IEEE Access 6:23053–23064. https://doi.org/10.1109/ACCESS.2018.2823765
25. Zhang T (2019) A novel approach of analog circuit fault diagnosis utilizing RFT noise estimation. Analog Integr Circuits Signal Process 98:517–526. https://doi.org/10.1007/s10470-018-1351-x
26. Zhao G, Liu X, Zhang B, Liu Y, Niu G, Hu C (2018) A novel approach for analog circuit fault diagnosis based on Deep Belief Network. Measurement 121:170–178. https://doi.org/10.1016/j.measurement.2018.02.044

Yuling Shang is currently a professor in Guilin University of Electronic Technology in China. She received her Ph.D. in Circuits and Systems from Xidian University in 2010. Her research interests focus on the signal integrity, fault diagnosis, and testing techniques.

Songyi Wei Graduated from Guilin University of Electronic Technology. He is currently pursuing a Master's degree in Electronic Information at Guilin University Of Electronic Technology. He is also engaged in integrated electronic circuit testing research.

Chunquan Li is a professor in Guilin University of Electronic Technology. He received his Ph.D. in Mechanical Engineering from Shanghai University in 2010. He has authored over 40 professional and scholarly publications in famous international journals or international conferences in the specialized fields of the microelectronics manufacturing technology and advanced manufacturing technology.

Xiaojing Ye is currently a Master of Engineering candidate in Guilin University of Electronic Technology, China. Her research interests focus on integrated circuit test.

Lizhen Zeng is a teacher in Guilin University of Electronic Technology, China. Her research interests focus on integrated circuit test.

Wei Hu is currently a Master of Engineering candidate in Guilin University of Electronic Technology, China. His research interests focus on dynamic obstacle avoidance for mobile robot.

Xiang He is currently a Master of Engineering candidate in Guilin University of Electronic Technology, China. His research interests focus on optical device on chip.

Jinzhuo Zhou is currently a Master of Engineering candidate in Guilin University of Electronic Technology, China. Her research interests focus on optical device on chip.